Published by IOP Publishing for Sissa Medialab

Received: *October 15, 2019*
Revised: *December 5, 2019*
Accepted: *January 7, 2020*
Published: *February 14, 2020*

21st International Workshop on Radiation Imaging Detectors
7–12 July 2019
Crete, Greece

Evaluation of scan strategies for small animal in vivo micro-CT

J. Dudak,[a] **D. Ekendahl,**[b] **L. Judas,**[b] **J. Mrzilkova,**[c] **P. Rubovic,**[a] **P. Zach**[c] **and J. Zemlicka**[a,1]

[a] *Institute of Experimental and Applied Physics, Czech Technical University in Prague, Husova 240/5, 110 00 Prague, Czech Republic*
[b] *National Radiation Protection Institute, Bartoskova 1450/28, 140 00 Prague, Czech Republic*
[c] *3rd Faculty of Medicine, Charles University in Prague, Ruska 2411/87, 100 00 Prague, Czech Republic*

E-mail: jan.zemlicka@utef.cvut.cz

Abstract: The micro-CT scanners of the radiography laboratories at the Institute of Experimental and Applied Physics (IEAP) have been used many times for post mortem imaging of small animals. The systems are based on the Timepix detector technology and they can provide CT models with spatial resolution up to few micrometres for such samples. Until now the investigated samples were *ex vivo* organs or small animals and image quality was a key parameter of these scans. The transition to the *in vivo* measurement is connected with the limitation of the absorbed dose in the investigated sample.

Pilot measurements with the thermoluminescent dosimeters (TLD) were performed and the dose rate for a small rodent was estimated. This dose rate limits the maximal irradiation time for live specimens to tens of seconds to avoid immunosuppression or other irreversible biological damages.

Series of measurements were performed with PlastiMouse™ phantom using different acquisition parameters to evaluate best data acquisition strategy for given dose limits. The presented data refers to the relationship between exposure time recorded by the detector and the reconstructed micro-CT slices quality. Contrast-to-noise ratio was evaluated for 112 selected combinations of acquisition times and angular sampling. This covers a range of sample doses from 50 to 4500 mGy delivered during recorded exposure time.

Keywords: Computerized Tomography (CT) and Computed Radiography (CR); Dosimetry concepts and apparatus; Image reconstruction in medical imaging; X-ray detectors

[1] Corresponding author.

https://doi.org/10.1088/1748-0221/15/02/C02019

Contents

1 Introduction

X-ray micro computed tomography (micro-CT) become a valuable non-destructive tool for scientific research in past decade [1]. Current state-of-the-art laboratory micro-CT systems provide spatial resolution of several micrometres for large variety of inspected samples [2]. Our work presents results obtained with adapted MARS micro-CT system equipped with Quad Timepix detector [3]. This detection technology is now routinely used for *ex vivo* measurements in pre-clinical research [4].

Previously published studies focused on X-ray irradiation of rodents have concluded that a lethal radiation dose for a laboratory mouse is generally in range of 7–11 Gy [5] depending on the age and specie of the specimen. Such radiation dose causes complete myeloablation (bone marrow activity decrease). The referred level LD50/30 (a dose causing death of 50% of irradiated specimens within 30 days) is 5–7.6 Gy [6]. Such dose levels are obviously too high for practical micro-CT measurements. It was also reported that immunosuppression was observed in case of doses exceeding 500 mGy [5]. Based on [7] rodents are capable to recover from a dose of 250–500 mGy within a day. Although scans with the radiation dose of 16.2 mGy have been reported and standard radiation dose for micro-CT scan is reported to be 100–300 mGy [8, 9]. Such dose is non-lethal; however, it can already induce deterministic effects.

The absorbed dose becomes an important parameter closely connected with the achievable spatial and contrast resolution. The absorbed dose increases with downsizing of voxels as the same number of absorbed photons in each voxel is needed to keep a constant contrast. A dose of 250 mGy should be capable to provide 1% contrast resolution for 135 µm voxels based on published simulations [10]. Unfortunately, the dose raises up to 5 Gy for 65 µm voxels if the same contrast resolution is required.

2020 JINST 15 C02019

2 Instrumentation

The following paragraphs briefly describe the used micro-CT for small animals, the absorbed dose estimated for this system and the mouse phantom used for presented measurements.

2.1 Micro-CT small animal scanner

One of the micro-CTs at IEAP is dedicated for small animal imaging. The construction of the scanner is gantry based in order to prevent sample movement. The system equipped with 70 kV Kevex PXS11-8012 micro focus X-ray tube and Timepix Quad detector provides 25 mm large field of view and spatial resolution up to 28 μm. The detector is equipped with 300 μm thick common silicon sensor and aluminium filters can be placed in front of the sample to cut the low energy spectrum (based on sample thickness and composition). The used X-ray tube needs to be turned on permanently, even between projections as it takes few seconds to stabilize its output when powered on.

2.2 Dose estimation

The acceptable dose delivered during a micro-CT scan should not induce any irreversible changes to the living animal. The 70 kVp spectrum of the Kevex PXS11-8012 X-ray tube was modelled in SpekCalc [11] and initial beam filtration was estimated to 250 μm of aluminium. This reflects the thickness of used silicon sensor (300 μm) as well as average diameter and tissue composition of small animals (up to 25 mm of soft tissue, air bubbles and bones).

The average dose rate was measured using cylindrical polyethylene phantom (20 mm in diameter) filled with a thermoluminescent dosimetry (TLD) material in powdered form (type of MCP-7P, TLD Poland). The absorbed dose was estimated to 2.1 mGy per second for routinely used 70 kVp and 150 μA tube spectrum filtered by 250 μm of aluminium. This value leads to tolerable scan times in the range of 50–250 seconds (approx. 100–500 mGy in the terms of absorbed dose for the given geometry).

2.3 Plastimouse^{TM} ethical phantom

The experiments were carried out with the use of Plastimouse^{TM} phantom to maximize measurement reproducibility and to avoid unnecessary irradiation of living animals. This allowed us to scan the same sample for multiple times even with long acquisition times and fine angular step. The Plastimouse^{TM} phantom is created by the plastination process of a mouse and thus it represents true anatomy of a living animal [12].

3 Scanning strategies

The CT scan time is given by the time necessary for single projection and the number of projections taken for the measured dataset. Single projection time is a complex quantity depending on used detector and positioning system as it covers not only acquisition (live) time but also frame read-out time and sample manipulation between projections. Unfortunately, the dose is delivered to the sample during the whole scan as it is not viable to shut down the X-ray tube between individual

2020 JINST 15 C02019

projections in the case of micro-focus X-ray tubes. The time course of the CT scan can be described by the following formula:

$$ST = NP \times (AT + FRO + GM) \tag{3.1}$$

where ST stands for the scan time, NP is the number of projections defined by the ratio of the angular range (half or full rotation) and the angle step, AT is the acquisition time, FRO is the frame read-out time (approx. 200 ms for used detector) and GM is the time needed for gantry movement (600–900 ms depending on the angular step). The subsequent considerations will mainly address an ideal scenario in which the dose is accumulated only during the projections acquisition (both FRO and GM are negligible compared to AT). The formula (3.1) is then simplified to:

$$ST = NP \times AT \tag{3.2}$$

Acquisition time influences the quality (the photon statistics and consequently the signal-to-noise ratio) of individual projections and the number of projections defines angular sampling density used for the CT reconstruction. Their product determines the irradiation time, i.e. absorbed dose in our scenario.

4 Results

Series of measurements were taken to experimentally verify the data quality provided by the used micro-CT scanner with the scan time restrictions given by the dose limitations. Ethical issues connected with irradiation of live animal during the experiments were avoided by the use of Plastimouse^{TM} phantom.

4.1 Experimental evaluation of the sampling strategies

The phantom was scanned multiple times with different values of angular step and acquisition time per projection. 112 micro-CT datasets were created in the experiment combining angular sampling from 0.5° to 2° with acquisition time within range from 0.25 to 3 seconds per projection. All measurements were carried out using Timepix Quad detector with 300 µm thick common silicon sensor. Effective pixel size of acquired projections was set to 44 µm in all cases. Figure 1 shows comparison of the same dataset created with the highest dose (720 projections, acquisition time 3 s per projection, absorbed dose 4.5 Gy) and with the lowest dose (97 projections, acquisition time 250 ms per projection, absorbed dose 50 mGy). The low-dose image obviously suffers from higher image noise and presence of angular sampling artifacts degrading the contrast resolution especially in soft tissue. Even in this case, it is still possible to clearly visualize bone abnormalities such as fractures (lower row of figure 1).

4.2 Data evaluation

Figure 2 shows a region of interest (denoted by the green rectangle in figure 1) containing bone and several different soft tissue structures (skin, muscle, rectum, bladder and uterus) acquired with the absorbed dose between 50 and 500 mGy and with different angular sampling. The absorbed dose increases from left to right in each row covering noted dose ranges. Actual acquisition parameters of each presented dataset are denoted at the image in form "number of projections × angular step,

2020 JINST 15 C02019

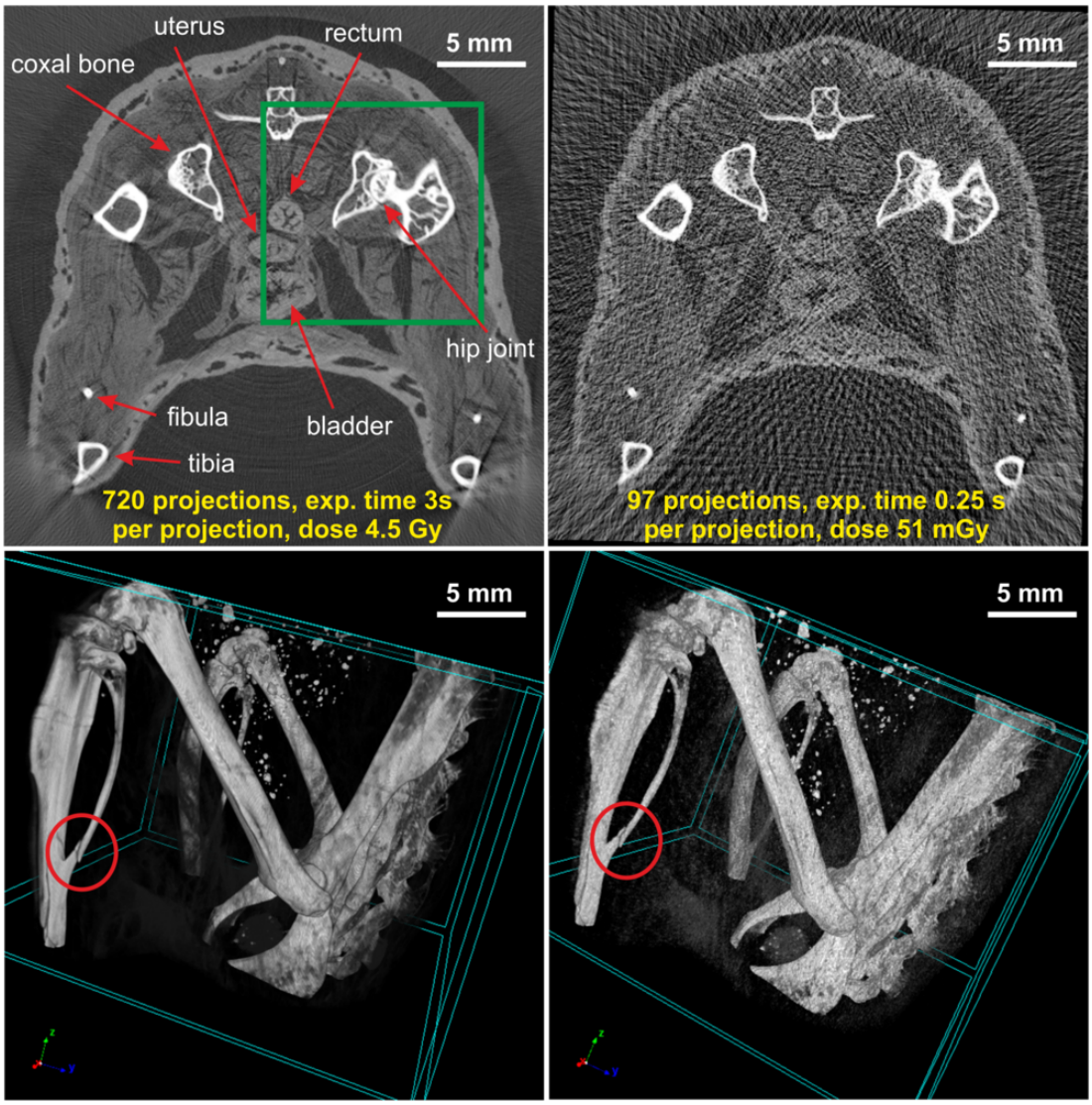

Figure 1. Comparison of the same slice (top row) and volume rendering of the skeleton (lower row) of the PlastiMouse^{TM} phantom scanned with total acquisition time of 2160 seconds (left) and 24.5 seconds (right). It is clearly visible that the low-dose data suffer from higher noise level and angular sampling artifacts but it is fully sufficient for visualization of bone fractures (denoted by red circles). The green rectangle, in the upper left image, shows the region of interest used for data quality evaluation.

acquisition time per projection". It can be observed that the noise level is indirectly proportional to the absorbed dose. It can be also noted that the detail detectability is generally better in the case of finer angular sampling. I.e. the fine structure of rectum is visualized with similar detail in figure 2 (i) and (o) although the latter was formed from data with reasonably higher absorbed dose.

The quality of obtained CT reconstructions was evaluated not only visually but also with the use of objective criterion of contrast-to-noise ratio (CNR) given by the followig formula:

$$\mathrm{CNR} = \frac{|I_1 - I_2|}{\sqrt{\sigma_1^2 + \sigma_2^2}} \tag{4.1}$$

2020 JINST 15 C02019

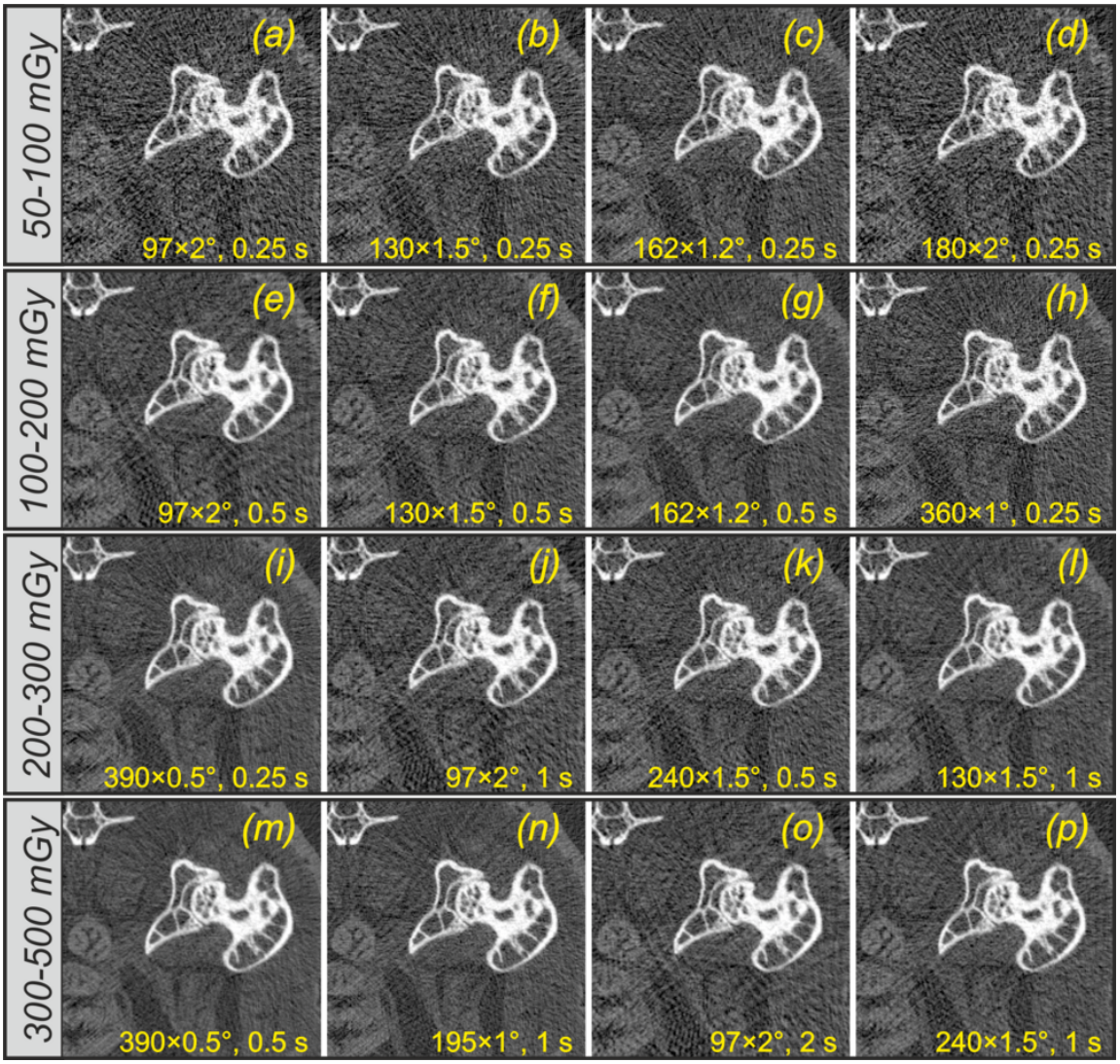

Figure 2. ROIs of a set of CT reconstructions acquired with absorbed dose within an interval of 50–500 mGy sorted in ascending order. The note at each image denotes "number of projections × angular step, acquisition time per projection". The noise level decreases with dose increase as can be expected. On top of that, the detail detectability within a "dose category" improves with reduction of the angle step.

where I_1 and I_2 are the intensities in two compared regions and σ_1 and σ_2 are their corresponding standard deviations. The regions of interest (ROI) within evaluated tissue types (bone, skin, muscle) were selected in a form of a square covering 400 voxels within a CT slice. The mean intensity and standard deviation of each ROI were calculated and used for the CNR estimation using the above-mentioned equation (4.1).

The value of CNR between skin and muscle (soft tissues) and bone and muscle can be plotted for different angular sampling and overall absorbed dose (see figure 3). Objects with CRN $>$ 3–5 (depending on shape and observer experience) are considered to be distinguishable according to Rose criterion [13]. Both plots clearly illustrate the dependence of the image quality on the angular sampling and the absorbed dose.

2020 JINST 15 C02019

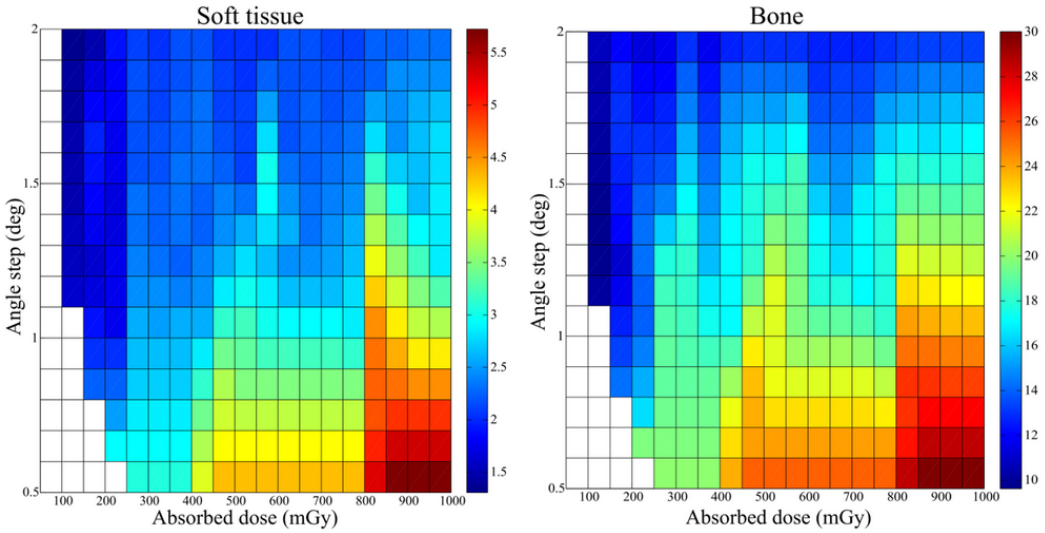

Figure 3. Contrast-to-noise ratio of soft tissue (left) and bone (right) with respect to the absorbed dose and the projection angle step. The unmeasured combinations are marked in white.

5 Discussion

The presented results are valid for an ideal micro-CT scanner characterized by the equation (3.2). As expected, presented data for current setup show that it is very easy to overcome CNR Rose criterion for bone structures even with the lowest absorbed doses (< 100 mGy). On the other hand, a dose higher than 800 mGy is needed for resolving skin and muscles according to this criterion. Therefore, it can be assumed that different types of soft tissue would not be resolvable using the tested detector. A significant part of the beam is not registered due to low quantum efficiency of used 300 µm thick silicon sensor. The detection efficiency of the sensor is only 22% for the used X-ray spectrum. Utilization of a different detector with higher sensor efficiency would further improve the imaging performance. Using 1 mm thick CdTe sensor would provide quantum efficiency exceeding 99% for the used 70 kVp spectrum. The comparable data quality as presented in figure 1 could be obtained using 4-times lower absorbed dose under such circumstances. Alternatively, the CNR could be improved while the same dose is conserved (i.e. the soft tissue CNR could fulfil the Rose criterion at dose level of 200 mGy).

The absorbed dose can be also reduced by properly set aluminium filter according to sample thickness and expected composition (mouse or rat size, used contrast agent etc.). The used micro-focus X-tube Kevex PXS11-8012 unfortunately needs several second for stabilization of a photon flux output when powered on. This means that the detector read-out time and gantry movement speed also contribute to absorbed dose because sample is irradiated even in time between projections (X-ray tube needs to be turned on during whole scan). Regrettably, impact of both mentioned sources of undesirable scan prolongation cannot be reduced without major changes of the used micro-CT setup.

Another possibility to overcome the described system limitations is to implement a synchronized fast X-ray beam shutter. This option should be independent on equipment and parameters of used system and it should bring us very close to the state that we defined as an ideal scenario in our reasoning.

2020 JINST 15 C02019

6 Conclusions

The tolerable absorbed dose for small animals lies in the range of 100–500 mGy depending on the investigated specimen. Measurements with such doses provide high enough CNR for bones but not for different types of soft tissues in the used micro-CT. Doses higher than 800 mGy are necessary for the differentiation of skin and muscle tissue with the spatial resolution below 50 µm. Dose reduction by factor of 4 can be achieved with 1 mm thick CdTe detector sensor for the same data quality. Implementation of fast X-ray beam shutter can minimize the dose absorbed in between projections even for current micro-CT setup.

Acknowledgments

The work was done in the frame of Medipix Collaboration and was financially supported from European Regional Development Fund-Project "Engineering applications of microworld physics" (No. CZ.02.1.01/0.0/0.0/16_019/0000766).

References

[1] J. Hsieh, *Computed tomography: principles, design, artifacts, and recent advances*, 2nd edition, SPIE Press, Bellingham, WA, U.S.A. (2009), ISBN 978-081-9475-336.

[2] S. Reza and K. Iniewski, *Semiconductor radiation detectors: technology and applications*, CRC Press, Boca Raton, FL, U.S.A. (2018), ISBN 978-113-8710-344.

[3] *Medipix website: A family of pixel detector read-out chips for particle imaging and detection developed by the Medipix Collaborations*, https://medipix.web.cern.ch.

[4] J. Dudak, J. Zemlicka, J. Karch, M. Patzelt, J. Mrzilkova, P. Zach et al., *High-contrast X-ray micro-radiography and micro-CT of ex-vivo soft tissue murine organs utilizing ethanol fixation and large area photon-counting detector*, *Sci. Rep.* **6** (2016) 30385.

[5] P. Dubé, *Considerations for rodent irradiation*, https://www.taconic.com/taconic-insights/oncology-immuno-oncology/rodent-irradiation-considerations.html.

[6] D. Cavanaugh, E. Johnson, R.E. Price, J. Kurie, E.L. Travis and D.D. Cody, *In vivo respiratory-gated micro-CT imaging in small-animal oncology models*, *Mol. Imag.* **3** (2004) 55.

[7] I. Willekens, N. Buls, T. Lahoutte, L. Baeyens, C. Vanhove, V. Caveliers et al., *Evaluation of the radiation dose in micro-CT with optimization of the scan protocol*, *Contrast Media Mol. I.* **5** (2010) 201.

[8] N. Miyahara, T. Kokubo, Y. Hara, A. Yamada, T. Koike and Y. Arai, *Evaluation of X-ray doses and their corresponding biological effects on experimental animals in cone-beam micro-CT scans (R-mCT2)*, *Radiol. Phys. Technol.* **9** (2015) 60.

[9] J.M. Boone, O. Velazquez and S.R. Cherry, *Small-animal X-ray dose from micro-CT*, *Mol. Imag.* **3** (2004) 149.

[10] N.L. Ford, M.M. Thornton and D.W. Holdsworth, *Fundamental image quality limits for microcomputed tomography in small animals*, *Med. Phys.* **30** (2003) 2869.

[11] G. Poludniowski, G. Landry, F. DeBlois, P.M. Evans and F. Verhaegen, *SpekCalc: a program to calculate photon spectra from tungsten anode X-ray tubes*, *Phys. Med. Biol.* **54** (2009) N433.

[12] Smart Scientific Solutions, *CT Imaging Phantoms PlastiCreatures*, http://www.smartscientificsolutions.com/products/.

[13] S.W. Smith, *The scientist and engineer's guide to digital signal processing*, California Technical Pub., San Diego, CA, U.S.A. (1997).

2020 JINST 15 C02019